Journal of Organometallic Chemistry 695 (2010) 2519–2525

Contents lists available at ScienceDirect

Journal of Organometallic Chemistry

journal homepage: www.elsevier.com/locate/jorganchem

# Ethynylferrocene insertion into Fe–C bond in bridging aminocarbyne diiron complexes: New triiron vinyliminium complexes

Luigi Busetto, Rita Mazzoni, Mauro Salmi, Stefano Zacchini, Valerio Zanotti*

*Dipartimento di Chimica Fisica e Inorganica, Università di Bologna, Viale Risorgimento 4, I-40136 Bologna, Italy*

## ARTICLE INFO

*Article history:*
Received 28 June 2010
Received in revised form
27 July 2010
Accepted 29 July 2010
Available online 6 August 2010

*Keywords:*
Vinyliminium
Aminocarbyne
Alkyne insertion
Ferrocene
Metallacycle
Diiron complexes

## ABSTRACT

The μ-aminocarbyne complexes $[Fe_2\{\mu\text{-}CN(Me)(R)\}(\mu\text{-}CO)(CO)(NCMe)(Cp)_2][SO_3CF_3]$ (R = Me, **1a**; Xyl, **1b**; Xyl = $2,6\text{-}Me_2C_6H_3$) react with ethynylferrocene to give the corresponding bridging vinyliminium complexes $[Fe_2\{\mu\text{-}\eta^1\text{:}\eta^3\text{-}C{=}N(Me)(R)CHC(Fc)\}(\mu\text{-}CO)(CO)(Cp)_2][SO_3CF_3]$ (R = Me, **2a**; R = Xyl, **2b**). Insertion of the ethynylferrocene in the metal–carbyne bond is regiospecific, and leads to the formation of only one isomer.

Complexes **2a** and **2b** undergo hydride addition (by $NaBH_4$) affording the enaminoalkylidene complex $[Fe_2\{\mu\text{-}\eta^1\text{:}\eta^3\text{-}C(H)(N(Me)_2)CHC(Fc)\}(\mu\text{-}CO)(CO)(Cp)_2]$ (**3a**) and the bis-alkylidene $[Fe_2\{\mu\text{-}\eta^1\text{:}\eta^2\text{-}C(N(Me)(Xyl))CH_2C(Fc)\}(\mu\text{-}CO)(CO)(Cp)_2]$ (**3b**), respectively. Upon treatment with NaH, compounds **2a** and **2b** undergo fragmentation, affording the 1-metalla-2-aminocyclopenta-1,3-dien-5-one complexes $[Fe(CO)(Cp)\{C(N(Me)(R))CHC(Fc)C(O)\}]$ (R = Me, **4a**; R = Xyl, **4b**).

The molecular structures of **2b**, **3b** and **4b** have been determined by X-ray diffraction studies.

## 1. Introduction

Metal-assisted C–C and C–heteroatom bond formation has a major role in the construction of highly complex molecular architectures [1]. Synthetic strategies also include the use of dinuclear (polynuclear) transition metal complexes, which take advantage of specific activation modes associated to multisite coordination, to promote the assembly of small and simple molecular units [2]. As an example, the assembly of bridging $C_1$ ligands (such as alkylidynes or alkylidenes) with alkenes or alkynes ($C_2$ units), provides an effective entry to the synthesis of bridging $C_3$ species [2a,3]. Within this field, we have shown that the diiron μ-aminoalkylidyne complexes **I** undergo insertion of alkynes into a metal–carbyne bond to form bridging vinyliminium complexes **II** (Scheme 1) [4].

The transformation shown in Scheme 1 is interesting for several reasons. First, insertion of a primary alkyne into the metal carbon bond is regiospecific: C–C bond formation occurs exclusively between the bridging alkylidyne carbon and the primary carbon of the alkyne. A second point is that the resulting bridging $C_3$ ligand is a α,β unsaturated iminium coordinated in a $\mu\text{-}\eta^1\eta^3$ mode. Conjugated iminiums are essential intermediates in iminium–enamine catalysis [5], and have a major role in the development of the organocascade catalysis [6]. However, as consequence of the bridging coordination, vinyliminium ligands display a unique and distinct reactivity compared to the corresponding non coordinated conjugated species [7]. A further significant aspect is that the observed C–C bond formation is assisted by iron, which is a cheap and environmental sustainable transition metal. This is of great interest in view of the growing demand for processes based on safe transition metal in the place of toxic and less abundant transition metals [8].

Based on these considerations, we decided to extend our studies to the insertion of ethynylferrocene in the metal alkylidyne carbon bond of **1**. The primary aim was to generate a bridging vinyliminium ligand connected to a further iron atom, in the form of ferrocenyl (Fc). Indeed, addition of ethynylferrocene to compounds and molecular arrays, including transition metal complexes [9], might significantly alter their nature and reactivity, due to the redox properties associated with the Fc group. The present work is intended to support these proposals.

## 2. Results and discussion

### 2.1. Insertion of ethynylferrocene into the iron–carbon bond of aminocarbyne complexes

The bridging aminocarbyne complexes $[Fe_2\{\mu\text{-}CN(Me)(R)\}(\mu\text{-}CO)(CO)(NCMe)(Cp)_2][SO_3CF_3]$ (R = Me, **1a**; Xyl, **1b**; Xyl = $2,6\text{-}Me_2C_6H_3$) react with ethynylferrocene, in refluxing $CH_2Cl_2$, to give the corresponding μ-vinyliminium complexes $[Fe_2\{\mu\text{-}\eta^1\text{:}\eta^3\text{-}C{=}N(Me)(R)CHC$

---

* Corresponding author. Tel.: +39 (0)512093695.
*E-mail address:* valerio.zanotti@unibo.it (V. Zanotti).

0022-328X/$ – see front matter © 2010 Elsevier B.V. All rights reserved.
doi:10.1016/j.jorganchem.2010.07.027

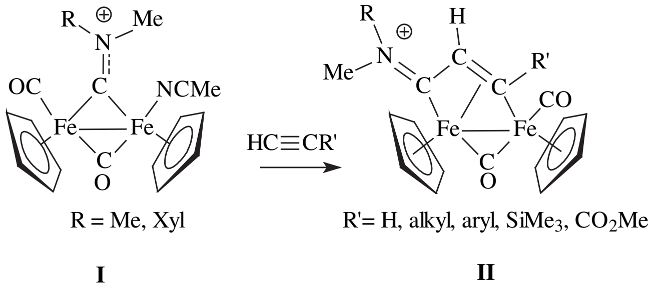

**Scheme 1.**

(Fc)}(μ-CO)(CO)(Cp)$_2$][SO$_3$CF$_3$] (R = Me, **2a**; R = Xyl, **2b**) in *ca.* 80% yields (Scheme 2).

In Scheme 2 the carbon atoms of the bridging chain have been labeled to make clearer the discussion and the considerations presented hereafter.

The reaction parallels those of **1** with simple organic alkynes (Scheme 1), with insertion into the metal carbon bond leading to the regiospecific formation of a vinyliminium ligand in which the Fc group is bound to the $C^3$ carbon of the bridging carbon chain.

Compounds **2a**,**b** were purified by chromatography on alumina and characterized by IR, NMR spectroscopy, and elemental analysis. Moreover, the molecular structure of **2b** has been determined by X-ray diffraction. The ORTEP diagram is shown in Fig. 1, and the main bond lengths and angles are reported in Table 1. The cation is composed by a *cis*-[Fe$_2$(μ-CO)(CO)(Cp)$_2$] to which is coordinated a bridging μ-η$^1$:η$^3$-C=N(Me)(Xyl)CHC(Fc) ferrocene-substituted vinyliminium ligand. All bonding parameters are as expected for this class of complexes [4], and the substituents at the iminium group display the usual *E*-conformation.

The NMR spectra of **2a**,**b** confirm that the reaction is regiospecific and leads to the formation of only one of the two possible isomers that insertion of a non-symmetric alkyne into the metal carbon bond might produce. Indeed, the CH portion of the inserted HC≡CFc generates a $^1$H NMR resonance at 4.70 ppm which is in the range expected for $C^2$–H [4], and is consistent with the geometry observed in the solid. The alternative isomer would have presented a $C^3$–H proton with a low field resonance, at about 11 ppm. Moreover, the NMR spectra (in CDCl$_3$) of **2b** show the presence of a significant NOE effect between the N-methyl and one Cp ring, demonstrating that **2b**, in solution, adopts the same *E*-configuration, with respect to the $C^1$=N double bond, that is observed in the solid. Finally, the resonances attributable to the ferrocenyl group are observed in the typical range at about 4–5 ppm. Relevant features in the $^{13}$C NMR spectra include the resonances due to the $C^1$, $C^2$ and $C^3$, in the range typical for vinyliminium ligands (*e.g.* for **2b**, at 231.7, 55.3 and 205.2 ppm, respectively). The IR spectra of **2a**,**b** (in CH$_2$Cl$_2$) show the expected *ν*(CO) band pattern consisting of one absorption for the terminal carbonyl (*e.g.* at 2001 cm$^{-1}$ for **2b**) and one for the bridging carbonyl (*e.g.* at 1817 cm$^{-1}$ for **2b**).

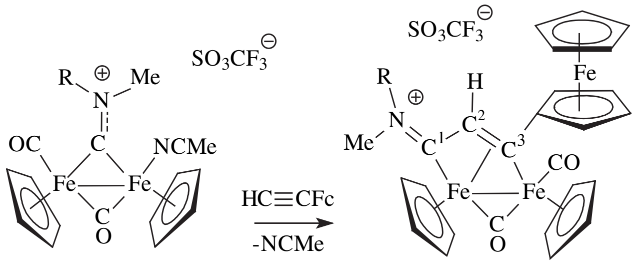

| | R | |
|---|---|---|
| **1a** | Me | **2a** |
| **1b** | Xyl | **2b** |

**Scheme 2.**

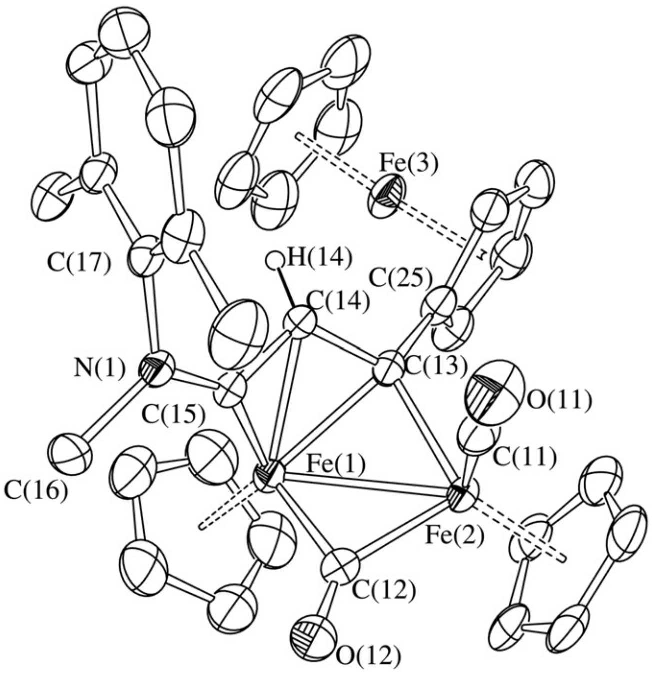

**Fig. 1.** Molecular structure of **2b** with key atoms labeled (all H-atoms, except H(14), have been omitted for clarity). Thermal ellipsoids are at the 30% probability level.

These results, together with previous results present clear evidence that the incorporation of alkynes into bridging

**Table 1**
Selected bond lengths (Å) and angles (°) for **2b** and **3b**.

| | **2b** | **3b** |
|---|---|---|
| Fe(1)–Fe(2) | 2.5552(10) | 2.5270(4) |
| Fe(2)–C(11) | 1.757(7) | 1.733(2) |
| Fe(1)–C(12) | 1.975(6) | 1.841(2) |
| Fe(2)–C(12) | 1.875(6) | 1.972(2) |
| Fe(1)–C(13) | 2.048(5) | 1.9788(18) |
| Fe(2)–C(13) | 1.962(5) | 2.0159(19) |
| Fe(1)–C(14) | 2.076(5) | 2.587(2) |
| Fe(1)–C(15) | 1.842(5) | 1.8830(19) |
| C(11)–O(11) | 1.137(7) | 1.148(3) |
| C(12)–O(12) | 1.171(7) | 1.186(3) |
| C(13)–C(14) | 1.412(6) | 1.537(3) |
| C(14)–C(15) | 1.427(7) | 1.492(3) |
| C(13)–C(25) | 1.484(7) | 1.480(3) |
| C(15)–N(1) | 1.301(6) | 1.316(2) |
| N(1)–C(16) | 1.479(7) | 1.468(3) |
| N(1)–C(17) | 1.458(6) | 1.453(3) |
| Fe(3)–Ct(1)[a] | 1.645(2) | 1.654(2) |
| Fe(3)–Ct(2)[b] | 1.664(2) | 1.657(2) |
| C(14)–C(13)–Fe(2) | 122.4(4) | 114.57(13) |
| C(13)–C(14)–C(15) | 118.4(4) | 95.34(14 |
| C(14)–C(15)–Fe(1) | 77.7(3) | 99.44(12) |
| C(14)–C(15)–N(1) | 132.2(4) | 121.88(17) |
| N(1)–C(15)–Fe(1) | 147.3(4) | 138.68(15) |
| C(15)–N(1)–C(16) | 121.1(4) | 121.68(17) |
| C(15)–N(1)–C(17) | 122.4(4) | 122.14(16) |
| C(17)–N(1)–C(16) | 116.4(4) | 116.17(16) |
| Fe(2)–C(13)–C(25) | 119.6(3) | 117.00(13) |
| C(14)–C(13)–C(25) | 116.3(4) | 114.68(16) |

[a] Ct(1) is the centroid of the substituted Cp-ring bonded to Fe(3).
[b] Ct(2) is the centroid of the unsubstituted Cp-ring bonded to Fe(3).

aminoalkylidyne units is general, and the presence of a ferrocenyl group, as alkyne substituent, modifies neither the reaction outcome, nor its regioselective character.

### *2.2. Reactions of the vinyliminium complexes with $NaBH_4$*

One of the most distinctive aspects of bridging vinyliminium complexes is the fact that they undergo nucleophilic addition at the iminium carbon ($C^1$) or at the adjacent α position ($C^2$), in the place of conjugated addition (addition at β position), which is typically observed in α,β unsaturated iminiums (non coordinated). A representative example is provided by hydride addition (from $NaBH_4$) [10]. Interestingly, the regiochemistry of the reaction is governed by the nature of the N substituent, in that the sterically demanding Xyl group generally acts as protecting group with respect to the iminium carbon, and directs hydride addition to the adjacent α position.

In theory, the presence of a Fc substituent might alter this reaction pattern, as a consequence of steric and electronic effects. In reality, we found that complexes **2a** and **2b** react with $NaBH_4$, leading to the formation of the complexes **3a** and **3b**, respectively (Scheme 3), in full agreement with the usual behavior of vinyliminium diiron complexes [10].

Compounds **3a**,**b** were purified by chromatography on alumina and characterized by spectroscopy, and elemental analysis. The molecular structure of **3b** was determined by X-ray diffraction. The ORTEP diagram is shown in Fig. 2, while the main bond lengths and angles are reported in Table 1. The geometry and bonding parameters of **3b** are in perfect agreement with those previously found for the closely related μ-vinylalkylidene complex $[Fe_2\{\mu\text{-}\eta^1:\eta^2\text{-}C(N(Me)(Xyl))CH_2C(COOMe)\}(\mu\text{-}CO)(CO)(Cp)_2]$ [10a]. As a consequence of hydride addition, C(14) is transformed into a saturated tetracoordinated carbon and the Fe(1)···C(14) contact [2.587(2) Å] becomes completely non-bonding. This breaks off the π-bond connection between the bridging alkylidene C(13) and the terminal alkylidene C(15) [C(13)–C(14) 1.537(3) Å; C(14)–C(15) 1.492(3) Å]. The terminal alkylidene function is stabilized by significant π-bond delocalization involving the nitrogen atom [C(15)–N(1) 1.301(6) Å; C(15)–Fe(1) 1.8830(19) Å].

The selective transformation of **2a** into **3a** is consistent with hydride addition occurring preferentially at the iminium carbon, with consequent transformation of the bridging vinyliminium into a stable μ-vinylalkylidene. Conversely, in the presence of the sterically demanding Xyl group (as in **2b**) $H^-$ addition is selectively directed to the $C^2$, with formation of the bis-alkylidene complexes **3b**.

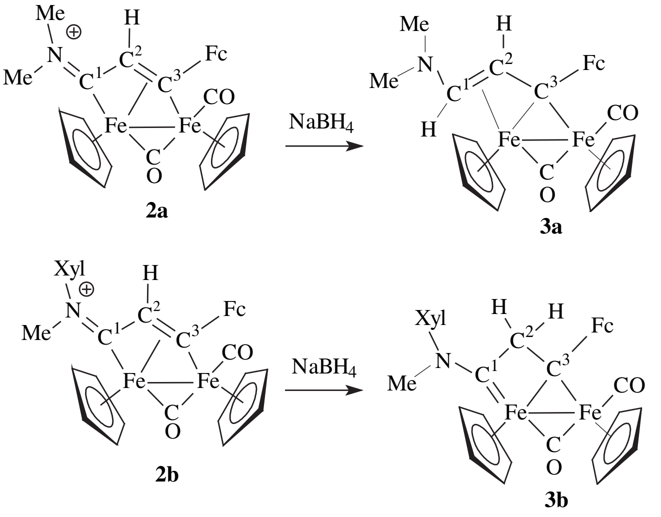

**Scheme 3.**

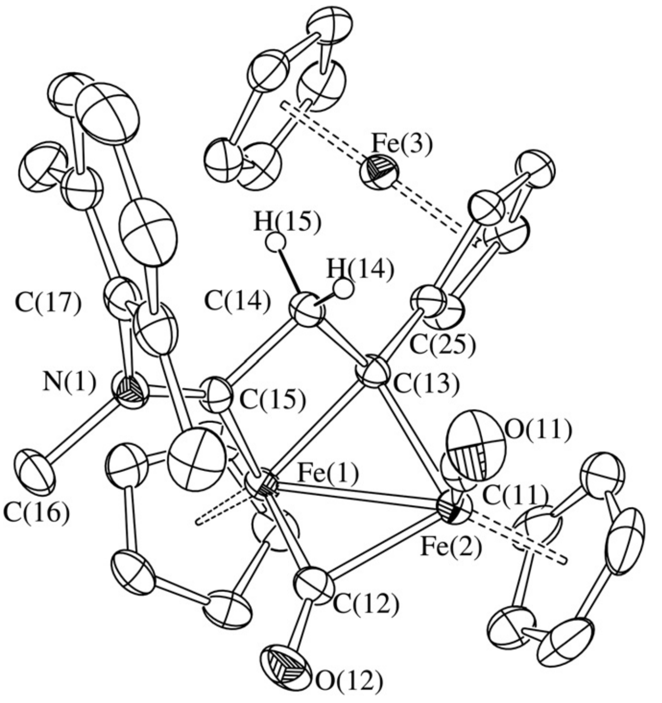

**Fig. 2.** Molecular structure of **3b** with key atoms labeled (all H-atoms, except H(14) and H(15), have been omitted for clarity). Thermal ellipsoids are at the 30% probability level.

NMR data are consistent with the above picture; in particular, both $^1H$ and $^{13}C$ NMR resonances of **3a** are very similar to that of analogous complexes previously reported, which simply contain a different group (*e.g.* Tol, $SiMe_3$, Me or $CH_2OH$) in the place of Fc [10a]. Most relevant features include the resonances of the $C^1H$ and $C^2H$ protons, that appear as doublets. Their coupling constant (of about 10 Hz) indicates that they are mutually *trans*, which correspond to an *E* configuration of the vinyl group. Therefore, the addition is both regio- and stereo-selective.

The NMR data of **3b** are similar to those of previously reported bis-alkylidene complexes of the type $[Fe_2\{\mu\text{-}\eta^1:\eta^2\text{-}C(R)CH_2CN(Me)(Xyl)\}(\mu\text{-}CO)(CO)(Cp)_2]$, containing the R group in the place of Fc (R = Tol, $SiMe_3$, Me, $CH_2OH$, COOMe, $Bu^n$, H) [10a]. The only remarkable difference between **3b** and the corresponding species that do not contain Fc, consists in the fact that these latter species are generally isomeric mixtures, with the *E* configuration predominant, but not exclusive (Scheme 4). Conversely, **3b** adopts exclusively the *E* configuration, as revealed by the presence of NOE effect between the N-methyl and one Cp ring. The isomeric forms are due to the orientation assumed by the different N substituents (Me and Xyl), as a consequence of the double bond character of the $C^1$–N interaction, and are in agreement with the aminocarbene nature of the ligand.

As for the alkyne insertion reaction (Scheme 2), the presence of Fc substituents does not change significantly the reaction profile concerning hydride addition, neither the geometry of the addition products.

### *2.3. Reactions of the vinyliminium complexes with NaH*

A further peculiar aspect of the bridging vinyliminium ligand, which is unusual for non coordinated α,β unsaturated iminium species, is the proton abstraction from the α position. The α C–H

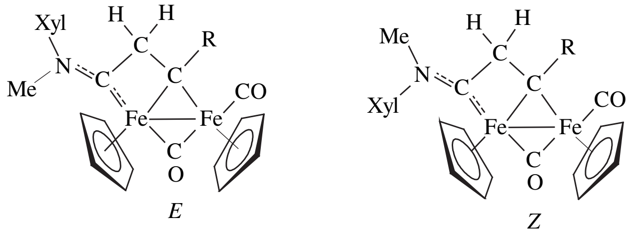

**Scheme 4.**

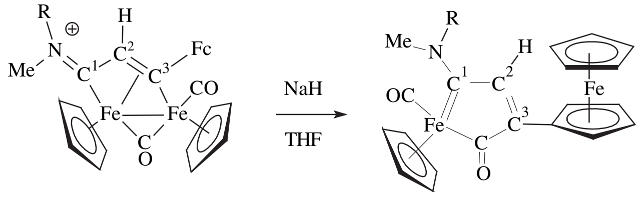

| | R | |
|---|---|---|
| **2a** | Me | **4a** |
| **2b** | Xyl | **4b** |

**Scheme 6.**

deprotonation leads to the formation of reactive intermediate species [11], which can be combined with a variety of reagents (*e.g.* elemental sulfur or selenium [12], diazoacetates [13], arylisocyanides [7b], and phenyldisulphides [14]), resulting in α C–H replacement with a range of functional groups (α-functionalization). Some of these functionalization reactions are shown in Scheme 5, as example.

In this case, the presence of a Fc substituent shows a relevant influence on the reaction outcome: we have found that complexes **2a**,**b**, upon treatment with NaH in the presence of elemental sulfur or $N_2CH(CO_2Et)$ do not react to form products analogous to **III** or **IV** (Scheme 5). Conversely, **2a**,**b** undergo fragmentation of the diiron unit, leading to the formation of metallacycle products **4a**,**b** (Scheme 6). The observed rearrangement is simply the consequence of the treatment with NaH, and does not involve reagents such as S or $N_2CHCO_2Et$, normally used to trap the deprotonated intermediate. Therefore, the products **4a**,**b** can be formed by reacting **2a**,**b** with NaH only (Scheme 6).

Compounds **4a**,**b** were obtained in about 70–75% yield after purification by column chromatography on alumina, and were characterized by IR and NMR spectroscopy, and elemental analysis. In addition, the molecular structure of **4b** has been determined by X-ray diffraction: the ORTEP diagram is shown in Fig. 3, while the main bond lengths and angles are reported in Table 2. The structure of **4b** is closely related to that previously reported for the 1-metalla-2-aminocyclopenta-1,3-dien-5-one complex [Fe(CO)(Cp){C(N(Me)(Xyl))CHC(Me)C(O)}] displaying very similar bonding parameters [11]. Thus, the five atoms constituting the metallacycle ring are almost coplanar (mean deviation from the Fe(1)–C(7)–C(8)–C(9)–C(10) least-squares plane 0.0480 Å). The Fe(1)–C(7) [1.908(2) Å] and Fe(1)–C(10) [1.935(2) Å] interactions are typical for a metal–aminocarbene and a metal–acyl; the former shows a strong π back-bonding, whereas the latter is mainly a σ interaction. Accordingly, the C(10)–O(2) interaction [1.216(3) Å] is an almost pure double bond, and also the aminocarbene C(7)–N(1) interaction [1.329(3) Å] shows a partial double bond character. The C–C interactions present an alternating behavior; thus, C(8)–C(9) [1.346(3) Å] is an almost pure double bond, whereas C(7)–C(8) [1.456(3) Å] and C(9)–C(10) [1.519(3) Å] are essentially single bonds. Finally, the aminocarbene nitrogen substituents adopt an *E* arrangement, as previously found for analogous complexes.

The spectroscopic data of **4a**,**b** are consistent with the structure found in the solid. In particular, the $^{13}C$ NMR spectra of **4a**,**b** (in $CDCl_3$), show the typical low-field resonances for the acyl carbon (*e.g.* at 268.7 ppm for **4b**) and for the aminocarbene carbon $C^1$ (*e.g.* at 262.2 ppm for **4b**). In agreement with the aminocarbene nature of the ligand, there is absence of free rotation around the $C^1$–N interaction due to the partial double bond character of the interaction. As a consequence, the two N-methyls in **4a** are non-equivalent, in the NMR time-scale, and give rise to distinct resonances. Likewise, NOE investigations indicate that the nitrogen substituents of **4b** adopt the *E* configuration, with respect to the $C^1$–N interaction, that is the same configuration observed in the solid.

Formation of the metallacyclic complexes **4a**,**b** is not unprecedented. In a restricted number of cases the treatment of vinyliminium complexes with NaH, in the absence of trapping reagents, leads to the formation of analogous cyclometallated products. In particular, complexes analogous to **4b** (containing Me, $CO_2Me$, $CMe_2OH$ in place of Fc) and a metallacycle compound similar to **4a**

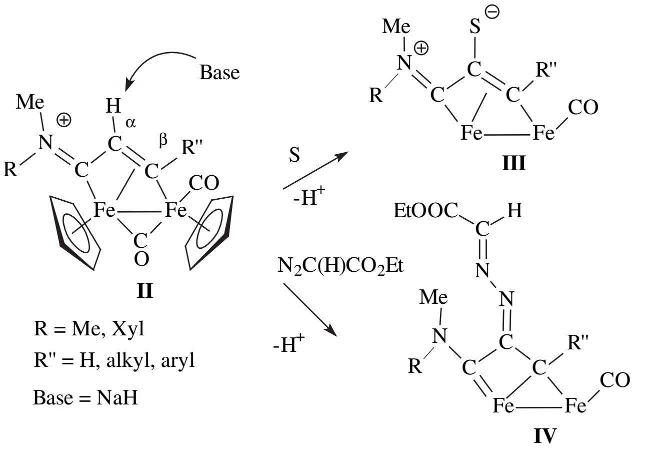

**Scheme 5.**

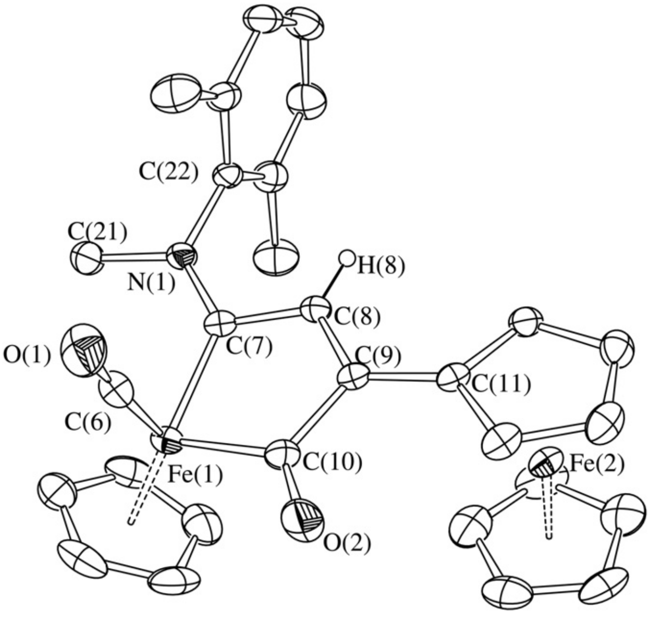

**Fig. 3.** Molecular structure of **4b** with key atoms labeled (all H-atoms, except H(8), have been omitted for clarity). Thermal ellipsoids are at the 30% probability level.

**Table 2**
Selected bond lengths (Å) and angles (°) **4b**.

| | | | |
|---|---|---|---|
| Fe(1)–C(6) | 1.727(3) | Fe(1)–C(7) | 1.908(2) |
| Fe(1)–C(10) | 1.935(2) | C(6)–O(1) | 1.155(3) |
| C(7)–C(8) | 1.456(3) | C(8)–C(9) | 1.346(3) |
| C(9)–C(10) | 1.519(3) | C(10)–O(2) | 1.216(3) |
| C(9)–C(11) | 1.455(3) | C(7)–N(1) | 1.329(3) |
| N(1)–C(21) | 1.465(3) | N(1)–C(22) | 1.450(3) |
| Fe(2)–Ct(1)[a] | 1.639(2) | Fe(2)–Ct(2)[b] | 1.652(2) |
| Fe(1)–C(7)–C(8) | 114.99(15) | C(7)–C(8)–C(9) | 115.62(19) |
| C(8)–C(9)–C(10) | 112.07(19) | C(9)–C(10)–Fe(1) | 113.32(15) |
| C(10)–Fe(1)–C(7) | 83.05(9) | C(9)–C(10)–O(2) | 119.9(2) |
| Fe(1)–C(10)–O(2) | 126.73(18) | C(8)–C(9)–C(11) | 124.51(19) |
| C(11)–C(9)–C(10) | 123.42(18) | Fe(1)–C(7)–N(1) | 128.33(16) |
| C(8)–C(7)–N(1) | 116.65(18) | C(7)–N(1)–C(21) | 122.45(19) |
| C(7)–N(1)–C(22) | 123.97(17) | C(22)–N(1)–C(21) | 113.55(17) |

[a] Ct(1) is the centroid of the substituted Cp-ring bonded to Fe(2).
[b] Ct(2) is the centroid of the unsubstituted Cp-ring bonded to Fe(2).

(containing a $Bu^n$ group in place of Fc) have been previously reported [11].

The metallacycle products clearly result from the assembly of the bridging vinyliminium ligand with a CO ligand, and do not require deprotonation. The reaction likely proceeds through a mechanism alternative to α C–H deprotonation, in which NaH does not remove the α C–H proton, but rather acts as reducing agent, favoring fragmentation of the dinuclear precursor and cyclization. The observed cyclization implies loss of a Fe containing fragment, formally corresponding to $[CpFe]^+$. We do not know the fate of the Fe fragment, that likely generates unidentified decomposition products, except for traces of $[Fe_2(CO)_4Cp_2]$, detected after chromatographic separation. The behavior of **2a,b** is peculiar, in that most of the vinyliminium complexes preferentially undergo deprotonation, upon treatment with NaH. The different behavior is presumably related to the presence of the ferrocenyl substituent: the redox properties of the Fc group might indeed favor reduction over deprotonation, thus affecting the reaction outcome. Unfortunately, the major consequence is the absence of reaction path leading to α CH replacement. On the other hand, complexes **4a**,**b** consist of a ferrocenyl unit having an unusual substituent: a metallacyclopentadienone. Indeed the design of new ferrocene-based molecular architectures [15] requires access to ferrocene complexes with unusual substituents on the cyclopentadienyl ring, which is mostly challenging, by a synthetic point of view [16].

Finally, since complexes **2a**,**b**, **3a**,**b**, and **4a**,**b** contain a ferrocenyl group, they have been also investigated by electrochemical methods. Electrochemical data were obtained from $10^{-3}$ M solutions in $CH_2Cl_2$ with $[Bu_4N][PF_6]$ 0.1 M. Cyclic voltammograms show reversible anodic peaks due to the ferrocenyl moiety. The potential values ($E_{1/2}$ in mV, referenced to the SCE, at a scan speed $\upsilon = 100\ mV\ s^{-1}$) are reported in the experimental part. Values are in a good agreement with the data reported for ethynylferrocenes [17].

## 3. Conclusions

Alkyne insertion into the metal carbon bond of bridging aminocarbyne ligands in diiron complexes has been successfully extended to ethynylferrocene. The resulting bridging vinyliminium fragment contains a ferrocenyl substituent in the β position. The reactivity of the vinyliminium complexes containing three iron centres closely resembles that of vinyliminium complexes obtained from purely organic alkynes, except for an higher tendency to undergo fragmentation and cyclization. New and unprecedented metallacycle complexes are consequently formed: they contain the Fc group as substituent on a five-member metallacycle.

All the reactions proceed in high yields and are almost completely selective.

## 4. Experimental details

### 4.1. General

All reactions were routinely carried out under a nitrogen atmosphere, using standard Schlenk techniques. Solvents were distilled immediately before use under nitrogen from appropriate drying agents. Chromatography separations were carried out on columns of deactivated alumina (4% w/w water). Glassware was oven-dried before use. Infrared spectra were recorded at 298 K on a Perkin–Elmer Spectrum 2000 FT-IR spectrophotometer and elemental analyses were performed on a ThermoQuest Flash 1112 Series EA Instrument. All NMR measurements were performed at 298 K on Mercury Plus 400 instrument. The chemical shifts for $^1H$ and $^{13}C$ were referenced to internal TMS. The spectra were fully assigned *via* DEPT experiments and $^1H,^{13}C$ correlation through gs-HSQC and gs-HMBC experiments [18]. NOE measurements were recorded using the DPFGSE-NOE sequence [19]. All the reagents were commercial products (Aldrich) of the highest purity available and used as received. $[Fe_2(CO)_4(Cp)_2]$ was purchased from Strem and used as received. Compounds **1a**,**b** were prepared by published methods [20].

### 4.2. Synthesis of $[Fe_2\{\mu\text{-}\eta^1:\eta^3\text{-}C{=}N(Me)(R)CHC(Fc)\}(\mu\text{-}CO)(CO)(Cp)_2][SO_3CF_3]$ (R = Me, **2a**; R = Xyl, **2b**)

A solution of **1a** (544 mg, 1.0 mmol) in $CH_2Cl_2$ (30 mL) was treated with ethynylferrocene (315 mg, 1.5 mmol). The reaction mixture was heated at reflux temperature for 4 h, then was allowed to cool to room temperature. Removal of the solvent and chromatography of the residue on an alumina column, with $CH_3OH$ as eluent, afforded a green/brown solid, corresponding to **2a**. Yield: 585 mg; 82%. Anal. Calcd. for $C_{28}H_{26}F_3Fe_3NO_5S$: C, 47.16; H, 3.67; N, 1.96. Found: C, 47.32; H, 3.54; N, 1.95%. IR ($CH_2Cl_2$) $\nu$(CO) 1989 (vs), 1807 (s); $\nu$(CN) 1686 (w) $cm^{-1}$. $^1H$ NMR ($CDCl_3$) $\delta$ 5.15 (s, 5H, Cp); 5.11 (s, 1H, $C^2H$); 4.81, 4.27 (s, 10H, Cp); 4.57, 4.50, 4.40, 4.30 (br m, 4H, $C^3{-}C_5H_4$); 3.80, 3.25 (s, 6H, NMe). $^{13}C\{^1H\}$ NMR ($CDCl_3$) $\delta$ 257.4 (μ-CO); 225.1 ($C^1$); 210.3 (CO); 201.2 ($C^3$); 91.4, 87.5 (Cp); 69.9 ($Cp_{Fc}$); 108.2, 72.4, 69.4, 68.1, 67.3 ($C^3C_5H_4$); 54.2 ($C^2$); 51.7, 44.7 (NMe) ppm.

Compound **2b** was prepared with the same procedure described for **2a**, by reacting **1b** with ethynylferrocene.

Crystals suitable for X-ray analysis were obtained by a dichloromethane solution, layered with diethyl ether, at −20 °C.

Compound **2b** (yield: 85%). Anal. Calcd. for $C_{35}H_{32}F_3Fe_3NO_5S$: C, 52.34; H, 4.02; N, 1.74. Found: C, 52.22; H, 4.14; N, 1.80%. IR ($CH_2Cl_2$) $\nu$(CO) 2001 (vs), 1817 (s); $\nu$(CN) 1628 (w) $cm^{-1}$. $^1H$ NMR ($CDCl_3$) $\delta$ 7.45–6.96 (m, 3H, $Me_2C_6H_3$); 5.37, 5.08 (s, 10H, Cp); 4.77 (s, 1H, $C^2H$); 4.72, 4.64, 4.40, 4.16 (m, 4H, $C^3{-}C_5H_4$); 4.26 (s, 3H, NMe); 4.12 (s, 5H, Cp); 2.38, 1.79 (s, 6H, $Me_2C_6H_3$). $^{13}C\{^1H\}$ NMR ($CDCl_3$) $\delta$ 254.2 (CO); 231.7 ($C^1$); 210.2 (CO); 205.2 ($C^3$); 145.4, 131.5, 129.8, 129.4 ($Me_2C_6H_3$); 92.2, 87.9 (Cp); 108.3, 72.2, 70.1, 68.7, 67.9 ($C^3{-}C_5H_4$); 69.6 ($Cp_{Fc}$); 55.3 ($C^2$); 46.1 ($NMe_2$); 18.1, 17.4 ($Me_2C_6H_3$) ppm.

### 4.3. Synthesis of $[Fe_2\{\mu\text{-}\eta^1:\eta^3\text{-}C(H)(NMe_2)CHC(Fc)\}(\mu\text{-}CO)(CO)(Cp)_2]$ (**3a**) and $[Fe_2\{\mu\text{-}\eta^1:\eta^2\text{-}C(N(Me)(Xyl))CH_2C(Fc)\}(\mu\text{-}CO)(CO)(Cp)_2]$ (**3b**)

A solution of **2a** (355 mg, 0.5 mmol) in THF (20 mL) was treated with $NaBH_4$ (93 mg, 2.5 mmol). The resulting mixture was stirred at room temperature for 60 min. Then, the solvent was removed under reduced pressure. The solid was re-dissolved in the minimal amount of $CH_2Cl_2$, then it was chromatographed through an alumina column, with $CH_2Cl_2$ as eluent, affording **3a**. Yield:

254 mg; 90%. Anal. Calcd. for $C_{27}H_{27}Fe_3NO_2$: C, 57.39; H, 4.82; N, 2.48. Found: C, 57.32; H, 4.62; N, 2.55%. IR ($CH_2Cl_2$) $\nu$(CO) 1927 (vs), 1750 (s) $cm^{-1}$. $^1H$ NMR ($CDCl_3$) $\delta$ 4.74 (br s, 5H, Cp); 4.70 (d, 1H, $C^2H$, $^3J_{HH} = 10.0$ Hz); 4.74, 4.52, 4.38, 4.33 (br s, $C^3{-}C_5H_4$); 4.34 (br s, 10H, Cp + $Cp_{Fc}$); 2.48 (s, 6H, $NMe_2$); 1.72 (d, 1H, $C^1H$, $^3J_{HH} = 10.0$ Hz). $^{13}C\{^1H\}$ NMR ($CDCl_3$) $\delta$ 278.8 ($\mu$-CO); 218.1 (CO); 177.2 ($C^3$); 104.8 ($C^1$); 87.9, 80.8 (Cp); 68.9 ($Cp_{Fc}$); 111.5, 72.2, 68.1, 67.5, 67.2 ($C^3C_5H_4$); 66.9 ($C^2$); 41.2 ($NMe_2$) ppm.

Compound **3b** was prepared with the same procedure described for **3a**, by reacting **2b** with $NaBH_4$. Crystals suitable for X-Ray diffraction were obtained by a $CH_2Cl_2$ solution, layered with hexane, at −20 °C.

Compound **3b** (yield: 91%). Anal. Calcd. for $C_{34}H_{33}Fe_3NO_2$: C, 62.33; H, 5.08; N, 2.14. Found: C, 62.21; H, 5.14; N, 2.03%. IR ($CH_2Cl_2$) $\nu$ (CO) 1919 (vs), 1738 (s) $cm^{-1}$. $^1H$ NMR ($CDCl_3$) $\delta$ 7.32–6.92 (m, 3H, $Me_2C_6H_3$); 4.81, 4.36, 4.23 (s, 15H, Cp); 4.43–4.26, 4.07 (m, 4H, $C^3C_5H_4$); 4.30 (d, 1H, $C^2H$, $^2J_{HH} = 20.0$ Hz); 3.72 (s, 3H, NMe); 3.35 (d, 1H, $C^2H$, $^2J_{HH} = 20.0$ Hz); 2.20, 1.92 (s, 6H, $Me_2C_6H_3$). $^{13}C\{^1H\}$ NMR ($CDCl_3$) $\delta$ 284.5 ($\mu$-CO); 271.7 ($C^1$); 219.7 (CO); 161.4 ($C^3$); 142.8, 129.2, 128.4, 128.3 ($Me_2C_6H_3$); 88.3, 85.3 (Cp); 74.3 ($C^2$); 69.0 ($Cp_{Fc}$); 115.8, 69.1, 66.8, 66.5, 65.5 ($C^3C_5H_4$); 45.9 (NMe); 17.9, 17.5 ($Me_2C_6H_3$) ppm.

### 4.4. *Synthesis of [Fe(CO)(Cp){C(N(Me)(R))CHC(Fc)C(O)}] (R = Me, **4a**; R = Xyl, **4b**)*

A solution of **2a** (355 mg, 0.5 mmol) in THF (20 mL) was treated with NaH (60 mg, 2.5 mmol). The resulting mixture was stirred at room temperature for 1 h. Then, it was filtered on an alumina pad. The solvent was then removed under reduced pressure. The solid was re-dissolved in the minimal amount of $CH_2Cl_2$, and passed through an alumina column, with $CH_2Cl_2$ as eluent, affording **4a**. Yield: 166 mg; 75%. Anal. Calcd. for $C_{22}H_{21}Fe_2NO_2$: C, 59.63; H, 4.78; N, 3.16. Found: C, 59.55; H, 4.69; N, 3.25%. IR ($CH_2Cl_2$) $\nu$(CO) 1910 (vs); $\nu$(CN) 1616 (m); $\nu(CO_{acyl})$ 1593 (m) $cm^{-1}$. $^1H$ NMR ($CDCl_3$) $\delta$ 7.50 (s, 1H, $C^2H$); 5.00, 4.73, 4.43, 4.40 (m, 4H, $C^3C_5H_4$); 4.53, 4.10 (s, 10H, Cp); 3.65, 3.47 (s, 6H, NMe). $^{13}C\{^1H\}$ NMR ($CDCl_3$) $\delta$ 270.1 ($CO_{acyl}$); 258.9 ($C^1$); 222.7 (CO); 172.9 ($C^3$); 141.4 ($C^2$); 85.4 (Cp); 75.0, 71.5, 71.0, 70.7, 68.9 ($C^3C_5H_4$); 70.2 ($Cp_{Fc}$); 51.7, 43.0 (NMe) ppm.

Compound **4b** was prepared with the same procedure described for **4a**, by reacting **2b** with NaH. Crystals suitable for X-ray diffraction were obtained from a $CH_2Cl_2$ solution, layered with hexane, at −20 °C.

Compound **4b** (yield: 72%). Anal. Calcd. for $C_{29}H_{27}Fe_2NO_2$: C, 65.32; H, 5.10; N, 2.63. Found: C, 65.38; H, 5.14; N, 2.63%. IR ($CH_2Cl_2$) $\nu$(CO) 1914 (vs); $\nu$(CN) 1625 (m); $\nu(CO_{acyl})$ 1596 (m) $cm^{-1}$. $^1H$ NMR ($CDCl_3$) $\delta$ 7.29–7.16 (m, 3H, $Me_2C_6H_3$); 6.74 (s, 1H, $C^2H$); 4.95, 4.40, 4.36, 4.30 (m, 4H, $C^3C_5H_4$); 4.67, 4.02 (s, 10H, Cp); 3.77 (s, 3H, NMe); 2.21, 2.17 (s, 6H, $Me_2C_6H_3$). $^{13}C\{^1H\}$ NMR ($CDCl_3$) $\delta$ 268.7 ($CO_{acyl}$); 262.2 ($C^1$); 222.1 (CO); 173.0 ($C^3$); 143.1 ($C^2$); 145.7, 132.9, 132.7 129.4, 129.1, 128.8 ($Me_2C_6H_3$); 85.3 (Cp); 74.6, 71.6, 71.0, 70.9, 68.7 ($C^3C_5H_4$); 70.2 ($Cp_{Fc}$); 48.7 (NMe); 17.9, 17.7 ($Me_2C_6H_3$).

### 4.5. *Electrochemical measurements*

Electrochemical data for **2a**,**b**, **3a**,**b** and **4a**,**b** were obtained from $10^{-3}$ M solutions in $CH_2Cl_2$ with $[Bu_4N][PF_6]$ 0.1 M ($E_{1/2}$ in mV, referenced to the SCE, at a scan speed $\upsilon = 100$ mV $s^{-1}$): **2a**, 560; **2b**, 553; **3a**, 529; **3b**, 534, **4a**, 511; **4b**, 507 mV.

### 4.6. *X-ray crystallography for **2b**, **3b**·$CH_2Cl_2$ and **4b***

Crystal data and collection details for are reported in Table 3. The diffraction experiments were carried out on a Bruker APEX II diffractometer equipped with a CCD detector using Mo-K$\alpha$ radiation. Data were corrected for Lorentz polarization and absorption effects (empirical absorption correction SADABS) [21]. Structures were solved by direct methods and refined by full-matrix least-squares based on all data using $F^2$ [22]. All hydrogen atoms were fixed at calculated positions and refined by a riding model, except H(14) in **2b**, H(14) and H(15) in **3b**·$CH_2Cl_2$, and H(8) in **4b** which were located in the Fourier map and refined isotropically using the 1.2 fold $U_{iso}$ value of the parent C-atoms. All non-hydrogen atoms were refined with anisotropic displacement parameters. Similar $U$ restraints were applied to the C-atoms (s.u. 0.005) in **2b**.

**Table 3**
Crystal data and experimental details for **2b**, **3b**·$CH_2Cl_2$ and **4b**.

| Complex | **2b** | **3b**·$CH_2Cl_2$ | **4b** |
|---|---|---|---|
| Formula | $C_{35}H_{32}F_3Fe_3NO_5S$ | $C_{35}H_{35}Cl_2Fe_3NO_2$ | $C_{29}H_{27}Fe_2NO_2$ |
| *Fw* | 803.23 | 740.09 | 533.22 |
| *T*, K | 296(2) | 295(2) | 296(2) |
| λ, Å | 0.71073 | 0.71073 | 0.71073 |
| Crystal system | Triclinic | Triclinic | Triclinic |
| Space group | $P\overline{1}$ | $P\overline{1}$ | $P\overline{1}$ |
| *a*, Å | 10.4304(16) | 10.4823(8) | 7.3663(11) |
| *b*, Å | 11.5864(18) | 11.8523(9) | 10.7966(15) |
| *c*, Å | 14.537(2) | 14.0455(11) | 16.091(2) |
| $\alpha$, ° | 97.155(2) | 98.2600(10) | 89.201(2) |
| $\beta$, ° | 102.884(2) | 93.9670(10) | 78.213(2) |
| $\gamma$, ° | 99.454(2) | 110.8180(10) | 77.453(2) |
| Cell volume, $Å^3$ | 1665.5(4) | 1600.5(2) | 1222.2(3) |
| *Z* | 2 | 2 | 2 |
| $D_c$, g $cm^{-3}$ | 1.602 | 1.536 | 1.449 |
| $\mu$, $mm^{-1}$ | 1.412 | 1.541 | 1.213 |
| *F*(000) | 820 | 760 | 552 |
| Crystal size, mm | 0.21 × 0.16 × 0.14 | 0.21 × 0.15 × 0.11 | 0.22 × 0.14 × 0.12 |
| $\theta$ limits, ° | 1.46–26.00 | 1.48–27.00 | 1.26–26.99 |
| Reflections collected | 16,416 | 17,889 | 13,704 |
| Independent reflections | 6504<br>[$R_{int} = 0.0302$] | 6937<br>[$R_{int} = 0.0195$] | 5293<br>[$R_{int} = 0.0279$] |
| Data/restraints/parameters | 6504/242/436 | 6937/0/397 | 5293/1/313 |
| Goodness on fit on $F^2$ | 1.061 | 1.030 | 1.002 |
| $R_1$ ($I > 2\sigma(I)$) | 0.0575 | 0.0319 | 0.0325 |
| $wR_2$ (all data) | 0.1800 | 0.0870 | 0.0823 |
| Largest diff. peak and hole, e $Å^{-3}$ | 0.747/−0.662 | 0.745/−0.550 | 0.293/−0.272 |

## Acknowledgement

We thank the Ministero dell'Università e della Ricerca Scientifica e Tecnologica (M.I.U.R.) (project: 'New strategies for the control of reactions: interactions of molecular fragments with metallic sites in unconventional species') and the University of Bologna for financial support.

## Appendix. Supplementary material

CCDC 782189, 782188 and 782190 for contain the supplementary crystallographic data for this paper. These data can be obtained free of charge from The Cambridge Crystallographic Data Centre via www.ccdc.cam.ac.uk/data_request/cif.

## References

[1] (a) E. Negishi, Bull. Chem. Soc. Jpn. 80 (2007) 233–257;
(b) K. Tamao, Top. Curr. Chem. 219 (2002) 1–9;
(c) A. de Meijere, F. Diederich (Eds.), Metal-Catalyzed Cross Coupling Reactions, second ed. Wiley-VCH, Weinheim, Germany, 2004;
(d) A. de Meijere, H. Hopf, Chem. Rev. 106 (2006) 4785–4786.

[2] (a) V. Ritleng, M.J. Chetcuti, Chem. Rev. 107 (2007) 797–858;
(b) M. Cowie, Can. J. Chem. 83 (2005) 1043–1055;
(c) S.A.R. Knox, J. Organomet. Chem. 400 (1990) 255–272;
(d) P. Braunstein, J. Rosè, in: P. Braunstein, L.A. Oro, P.R. Raithby (Eds.), Metal Cluster in Chemistry, Wiley-VCH, Weinheim, 1999;

R.A. Adams, F.A. Cotton (Eds.), Catalysis by Di- and Polynuclear Metal Cluster Complexes, Wiley-VCH, New York, 1998.
[3] L. Busetto, P. Maitlis, V. Zanotti, Coord. Chem. Rev. 254 (2010) 470–486 and references therein.
[4] V.G. Albano, L. Busetto, F. Marchetti, M. Monari, S. Zacchini, V. Zanotti, Organometallics 22 (2003) 1326–1331.
[5] (a) A. Erkkilä, I. Majander, P.M. Pihko, Chem. Rev. 107 (2007) 5416–5470;
(b) S. Mukherjee, J.W. Yang, S. Hoffmann, B. List, Chem. Rev. 107 (2007) 5471–5569;
(c) B. List, Acc. Chem. Res. 37 (2004) 548–557;
(d) B. List, R.A. Lerner, C.F. Barbas III, J. Am. Chem. Soc. 122 (2000) 2395–2396.
[6] Selected reviews include: (a) B. Simmons, A.M. Walji, D.W.C. MacMillan, Angew. Chem., Int. Ed. 48 (2009) 4349–4353;
(b) D. Enders, C. Grondal, M.R.M. Hüttl, Angew. Chem., Int. Ed. 46 (2007) 1570–1581;
(c) P. Melchiorre, M. Marigo, A. Carlone, G. Bartoli, Angew. Chem., Int. Ed. 47 (2008) 6138–6171;
(d) B. List, Chem. Commun. 8 (2006) 819–824.
[7] See for example: (a) L. Busetto, F. Marchetti, S. Zacchini, V. Zanotti, Eur. J. Inorg. Chem. (2007) 1799–1807;
(b) L. Busetto, F. Marchetti, S. Zacchini, V. Zanotti, Organometallics 27 (2008) 5058–5066.
[8] (a) B. Plietker (Ed.), Iron Catalysis in Organic Chemistry, Wiley-VCH, Weinheim, 2008;
(b) S. Enthaler, K. Junge, M. Beller, Angew. Chem., Int. Ed. 47 (2008) 3317–3321;
(c) A. Correa, O.G. Mancheño, C. Bolm, Chem. Soc. Rev. 37 (2008) 1108–1117;
(d) B.D. Sherry, A. Fürstner, Acc. Chem. Res. 41 (2008) 1500–1511;
(e) R.M. Bullock, Angew. Chem., Int. Ed. 46 (2007) 7360–7363.
[9] See for example: (a) D.-H. Wu, C.-H. Wu, Y.-Z. Li, D.-D. Guo, X.-M. Wang, H. Yan, Dalton Trans. (2009) 285–290;
(b) A. Albinati, F. Fabrizi de Biani, P. Leoni, L. Marchetti, M. Pasquali, S. Rizzato, P. Zanello, Angew. Chem., Int. Ed. 44 (2005) 5701–5705;
(c) W.-Y. Wong, K.-Y. Ho, K.-H. Choi, J. Organomet. Chem. 670 (2003) 17–26;
(d) U. Siemeling, J. Vorder BrKggen, U. Vorfeld, B. Neumann, A. Stammler, H.-G. Stammler, A. Brockhinke, R. Plessow, P. Zanello, F. Laschi, F. Fabrizi de Biani, M. Fontani, S. Steenken, M. Stapper, G. Gurzadyan, Chem.—Eur. J 9 (2003) 2819–2833;
(e) C. Lebreton, D. Touchard, L. Le Pichon, A. Daridor, L. Toupet, P.H. Dixneuf, Inorg. Chim. Acta 272 (1998) 188–196.
[10] (a) V.G. Albano, L. Busetto, F. Marchetti, M. Monari, S. Zacchini, V. Zanotti, Organometallics 23 (2004) 3348–3354;
(b) V.G. Albano, L. Busetto, F. Marchetti, M. Monari, S. Zacchini, V. Zanotti, J. Organomet. Chem. 690 (2005) 837–846.
[11] L. Busetto, F. Marchetti, S. Zacchini, V. Zanotti, Organometallics 24 (2005) 2297–2306.
[12] L. Busetto, F. Marchetti, S. Zacchini, V. Zanotti, Organometallics 25 (2006) 4808–4816.
[13] L. Busetto, F. Marchetti, S. Zacchini, V. Zanotti, Organometallics 26 (2007) 3577–3584.
[14] L. Busetto, F. Marchetti, R. Mazzoni, M. Salmi, S. Zacchini, V. Zanotti, J. Organomet. Chem. 693 (2008) 3191–3196.
[15] For a comprehensive overview of ferrocene see: (a) A. Togni, T. Hayashi (Eds.), Ferrocenes: Homogeneous Catalysis – Organic Synthesis – Materials Science, Wiley-VCH, Weinheim, 1995;
(b) A. Togni, R.L. Halterman (Eds.), Metallocenes, Wiley-VCH, Weinheim, 1998;
(c) P. Štěpnička (Ed.), Ferrocenes; Ligands Materials and Biomolecules, John Wiley & Sons, West Sussex, 2008.
[16] (a) A.H. Stoll, P. Mayer, P. Knochel, Organometallics 26 (2007) 6694–6697;
(b) Y. Wang, W. Weissensteiner, F. Spindler, V.B. Arion, K. Mereiter, Organometallics 26 (2007) 3530–3540;
(c) P. Christophe, B. Odell, J.M. Brown, Chem. Commun. (2004) 598–599;
(d) M. Steurer, K. Tiedl, Y. Wang, W. Weissensteiner, Chem. Commun. (2005) 4929–4931;
(e) D.C.D. Butler, C.J. Richards, Organometallics 21 (2002) 5433–5436;
(f) D. van Leusen, B. Hessen, Organometallics 20 (2001) 224–226;
(g) C. Metallinos, J. Zaifman, L. Dodge, Org. Lett. 10 (2008) 3527–3530.
[17] H. Fink, N.J. Long, A.J. Martin, G. Opromolla, A.J.P. White, D.J. Williams, P. Zanello, Organometallics 16 (1997) 2646–2650.
[18] W. Wilker, D. Leibfritz, R. Kerssebaum, W. Beimel, Magn. Reson. Chem. 31 (1993) 287–292.
[19] K. Stott, J. Stonehouse, J. Keeler, T.L. Hwang, A.J. Shaka, J. Am. Chem. Soc. 117 (1995) 4199–4200.
[20] G. Cox, C. Dowling, A.R. Manning, P. McArdle, D. Cunningham, J. Organomet. Chem. 438 (1992) 143–158.
[21] G.M. Sheldrick, Sadabs, Program for Empirical Absorption Correction. University of Göttingen, Germany, 1996.
[22] G.M. Sheldrick, SHELX97, Program for Crystal Structure Determination. University of Göttingen, Germany, 1997.